Supporting Information

A High-Energy-Density Rechargeable Mg Battery Enabled by Displacement Reaction

*Minglei Mao,†‡ ∥ Tao Gao,† ∥ Singyuk Hou,† Fei Wang,† Ji Chen,† Zengxi Wei,‡ Xiulin Fan,† Xiao Ji,† Jianmin Ma,‡ and Chunsheng Wang†**

†Department of Chemical and Biomolecular Engineering, University of Maryland, College Park, MD 20742 (USA)

‡School of Physics and Electronics, Hunan University, Changsha, 410082, China

Experimental section

Preparation of CuS microspheres: In a typical procedure, $CuSO_4 \cdot 5H_2O$ (2.5 mmol) (Alfa Aesar, 99%) and equimolar $Na_2S_2O_3 \cdot 5H_2O$ (Alfa Aesar, 99.5%) were put into a Teflon-lined stainless steel autoclave (50 ml), to which deionized water (40 mL) was added with stirring to form a yellowish homogeneous solution. The autoclave was sealed and maintained at 150 °C for 12 h, then allowed to cool down to room temperature naturally. The precipitates were collected by centrifugation, washed with deionized water and ethanol, and dried in a vacuum oven at 80 °C overnight. The composites were annealed in a conventional tube furnace at 350 °C for 2 h in a stream of argon flowing at 200 sccm. The commercial CuS (Alfa Aesar, 99.98%) was used as received without any further purification.

Material Characterizations: Hitachi (Tokyo, Japan) SU-70 HR-SEM was used to characterize the morphologies and size of the synthesized samples. The chemical composition was investigated by the energy dispersive spectroscopy (EDS). Transmission electron microscope (TEM) graphs were determined by JEOL ARM 200F. X-ray powder diffraction (XRD) patterns were recorded on a Bruker Smart1000 diffractometer with a Cu Kα radiation. X-ray photoelectron spectroscopy (XPS) were collected at room temperature with an XPS spectrometer (Thermo Scientific ESCALAB 250Xi) using monochromic AlKa radiation. The Brunauer−Emmett−Teller (BET) measurements were carried out using a Micromeritics ASAP 2020 system. Inductively coupled plasma (ICP) analysis was conducted with a ICP Perkin-Elmer Optima 3000 DV. For ex situ XPS measurements, coin cells were disassembled in an argon-filled glove box and the electrodes were washed with DME (anhydrous, Alfa Aesar, 99.9%) for three times to

remove the electrolyte, then the drying samples were obtained and moved to Argon-filled sealing tube as transferred box. In this process, all samples were exposed to air within 3-4s.

Electrochemical Measurements: Cell assembly was carried out in an Ar-filled glovebox with O_2 and H_2O levels below 0.1 ppm. CuS electrodes were prepared by compressing the as-prepared CuS powders, PTFE, carbon black at a weight ratio of 8:1:1 onto the molybdenum grid. Electrochemical performance was tested in pouch cells, with MACC as the electrolyte,[1] polished Mg metal as the anode, and glass fiber as separators. The MACC electrolyte was synthesized following the reported procedure,[1] with DME as the solvent. In a typical preparation of an electrochemically active MACC solution, $MgCl_2$ (Sigma, 99.99%) and $AlCl_3$ powder (Sigma, 99.999%) with the same molar ratio were added into DME (anhydrous, Alfa Aesar, 99.9%). Then, the solution was heated to above 30 °C for overnight with constant stirring. After returned to room temperature, the transparent MACC electrolyte is formed without any precipitation. The electrochemistry was conducted on Arbin battery test station (BT2000, Arbin Instruments, USA) at 5 mA/g with voltage cutoff of 0.5-2.2 V, with cells held in a thermostatted oven at room temperature. During GITT measurement, the electrode was discharged/charged at a pulse current of 5 mA/g for a duration of 2 h, followed by a relaxation of 8h at open circuit to reach equilibrium potentials. Nyquist plots were recorded using a Gamry 1000E electrochemical workstation (Gamry Instruments, USA) at a frequency range of 0.01-100 kHz. The linear sweep voltammetry (LSV) were carried out in a three-electrode cell on a CHI660D electrochemical workstation. The three-electrode cell consisted of a working electrode (Mo and SS 316L purchased from Aldrich), a counter electrode (Mg purchased

from Aldrich), a reference electrode (Mg), and the MACC electrolyte. During LSV analyses conducted on the selected current collectors, the scan potential was controlled from open circuit potential (OCP) to 3 V at the scan rate of 0.5 mV/s.

Theoretical equilibrium voltage ($V_{equilibrium}$) is calculated by

$$2CuS + Mg \rightarrow Cu_2S + MgS \qquad \Delta H_{experimental} = -321\,kJ/mol$$ [2-3]

$$Cu_2S + Mg \rightarrow 2Cu + MgS \qquad \Delta H_{experimental} = -266\,kJ/mol$$

$$V_{equilibrium} = -\frac{\Delta H}{nF}$$

$\Delta H_{experimental}$ is the reaction enthalpy. n is the number of electron transferred. F is the faraday's constant (96485 C/mol).

The theoretical capacity of CuS ($C_{theoretical}$=560 mA h/g) is calculated by:

$$C_{theoretical} = \frac{nF}{3.6M}$$
$$= \frac{2*96485}{3.6*95.6} mAh/g$$
$$= 560 mAh/g$$

n is the number of electron transferred (n=2). F is the Faraday's constant (F=96485 C/mol). M is the relative molecular mass (M=95.6 g/mol).

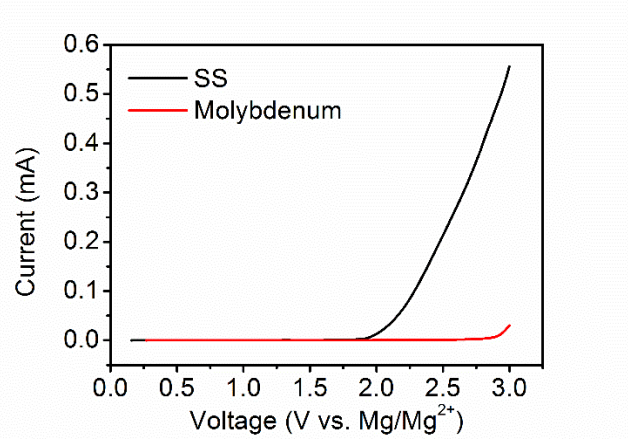

Figure S1. Linear sweep voltammograms of SS 316L and Mo grid in MACC electrolyte within the potential range between OCV and 3 V (vs. Mg/Mg^{2+}) collected at the scan rate of 1 mV/s.

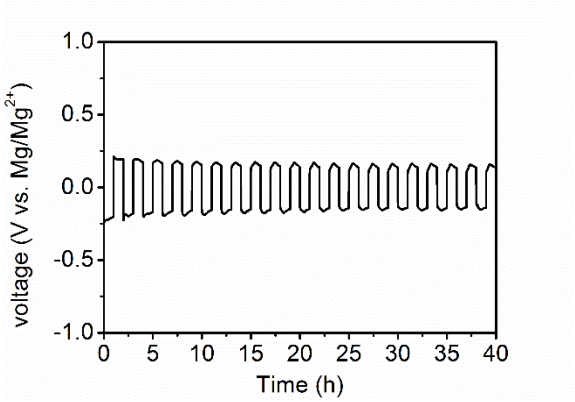

Figure S2. Typical Mg deposition and stripping with MACC electrolyte in a symmetrical Mg/Mg cell at a current density of 0.1 mA/cm^2. Overpotential: ~0.1 V.

Though APC is the most commonly used electrolyte for Mg batteries, it cannot be used in sulfides, because phenylmagnesium chloride is not compatible with sulfur, and the polysulfides are readily dissolved in the solvent THF of APC, causing the rapid drop of capacities.[4] In addition, the overpotential for Mg stripping/plating is (~0.1V at a current density of 0.1 mA/cm^2) lower than those of other Mg battery electrolytes.[5] Besides, the procedure to synthesize MACC electrolyte is simple.

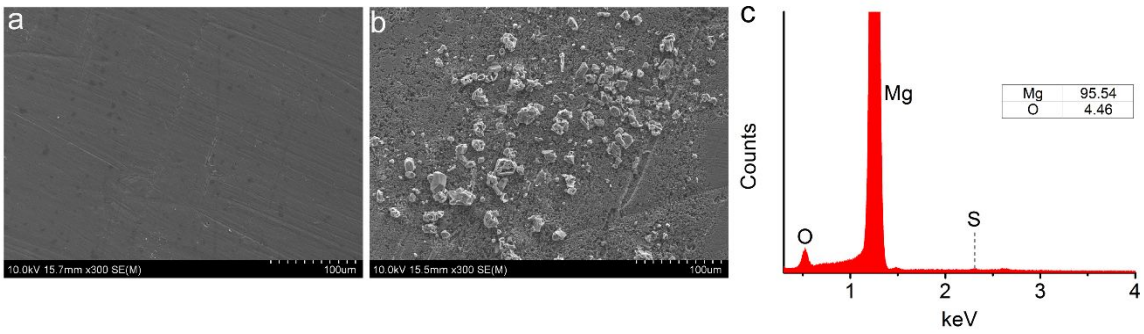

Figure S3. Morphology of (a) pristine, (b) cycled Mg electrodes. (c) Energy Dispersive X-ray Spectra (EDS) of cycled Mg anode. No sulfur peak is found.

The morphology of pristine and cycled Mg anode is presented in Figure S3a and b, in which the surface of pristine Mg is flat and smooth, while there are micro-sized particles on the surface of cycled Mg, because of stripping/plating of Mg. In EDS spectra for cycled Mg (Figure S3c), there are strong peaks of Mg and a small peak of oxygen, because of some inevitable oxide films. However, there is no peak for sulfur on the surface of cycled Mg, indicating no transport of Mg sulfide to the Mg anode.

Table S1. The electrochemical performance of typical cathodes reported for rechargeable Mg batteries.

Materials	Capacity (mA h/g)	Potential	Cycle number	Temperature
Chevrel phase[6]	110	1.1 V	2000	RT [a)]
Spinel Ti_2S_4[7]	140	1.2 V	40	60 °C
Layered TiS_2[8]	115	~1 V	40	60 °C
$TiSe_2$[9]	108	~1 V	50	RT
TiS_3[10]	83.7	~1.2 V	50	RT
Cu_2Se[11]	117	0.95 V	35	RT
CuS[12]	170	1.15 (0.5-1.8 V)	10	150 °C
CuS[13]	119	1.15 (0.5-1.8 V)	30	50 °C
This work	**335**	**1.52 V (0.5-2.2 V)**	**80**	**RT**

a) Room temperature

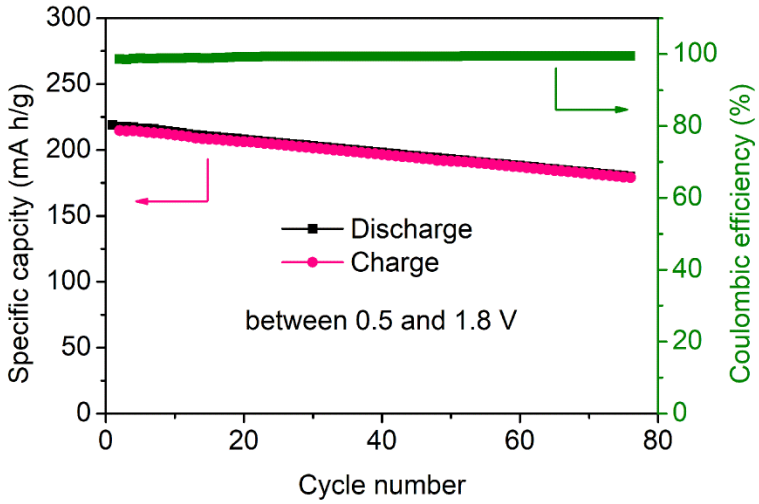

Figure S4. Cycling performance and coulombic efficiency (CE) of CuS/Mg pouch cells from 2nd to 75th cycles between 0.5-1.8V at 5 mA/g and RT.

To highlight the advantages of CuS second microspheres in this work, we also test CuS/Mg pouch cells at 0.5-1.8 V, the same voltage cutoff as other reported CuS. CuS second microspheres deliver an average capacity of 200 mA h/g within 75 cycles (Figure S4), much better than that of reported CuS both in capacity and cyclability (Table S1).

Table S2. The specifications of the CuS/Mg pouch cell with the dimensions reported by Aurbach et al.[14]

	Specification	Value
Cathode (CuS)	Reversible capacity Composition of active material Voltage Density (active + conductive + binder) Loading Swelling Thickness (both side coating) Number of stack	400 mA h/g 93 % 1.52 V vs. Mg/Mg^{2+} 3.79 g/cm^3 28.7 mg/cm^2 5 % 136.9 μm 47
Anode (Mg metal)	Reversible capacity Composition of active material Density Loading Swelling Thickness Number of stack	2205 mA h/g 100 % 1.74 g/cm^3 3.1 mg/cm^2 0 % 25 μm 48
Full Cell	Dimension n/p ratio (capacity based) Total capacity Voltage Energy density	300*100*10 mm^3 1.5 205.8Ah 1.52 V 1042 Wh/L

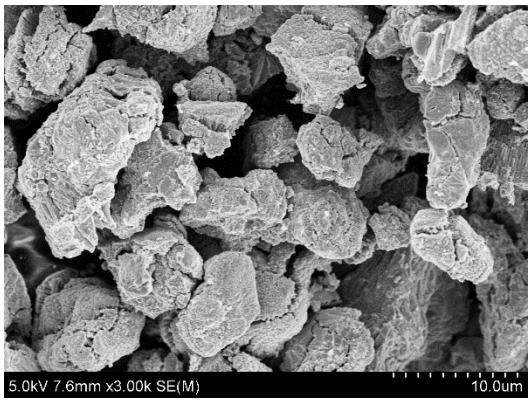

Figure S5. SEM image of commercial CuS.

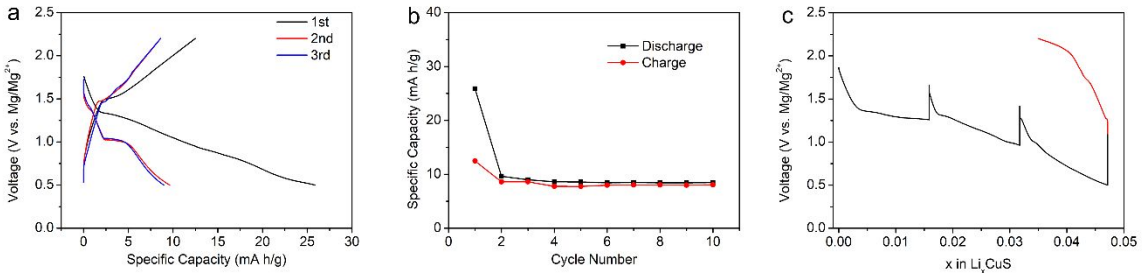

Figure S6. Electrochemistry performance of commercial CuS with an MACC electrolyte and a Mg negative electrode between 0.5 and 2.2 V at RT. (a) The discharge/charge curves of the first three cycles at the current density of 5 mA/g. (b) Cycling performance of the first 10 cycles at a current density of 5 mA/g. (c) Quasi-equilibrium voltage profile of commercial CuS/Mg system obtained from GITT. The cells were allowed to relax for 8 h after every 2 h discharging or charging at 5 mA/g and RT.

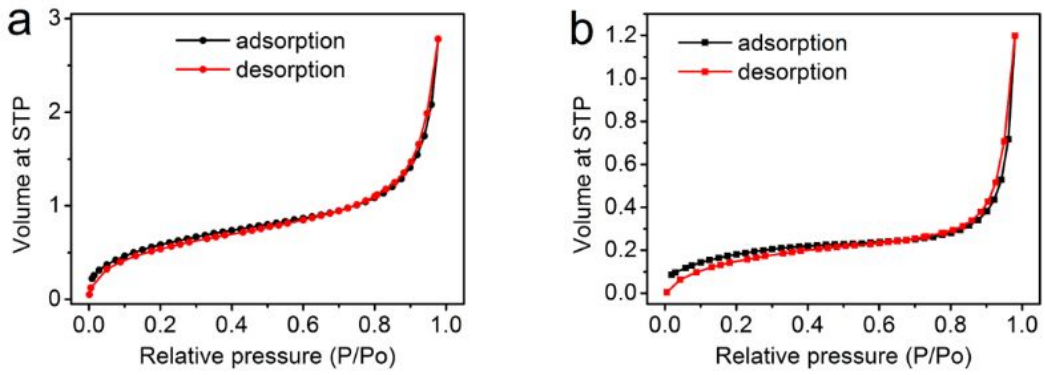

Figure S7. BET nitrogen adsorption and desorption isotherms of (a) CuS microspheres, (b) commercial CuS. The surface area for CuS microspheres and commercial CuS are 17870 and 5112 cm^2/g, respectively.

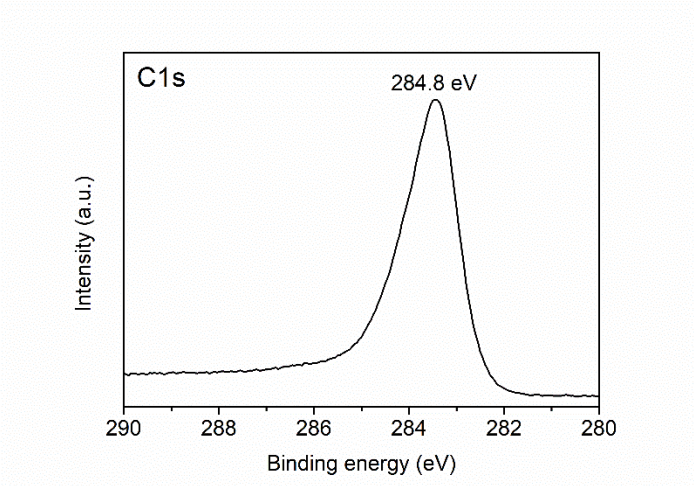

Figure S8. XPS C1s spectra of pristine CuS electrode.

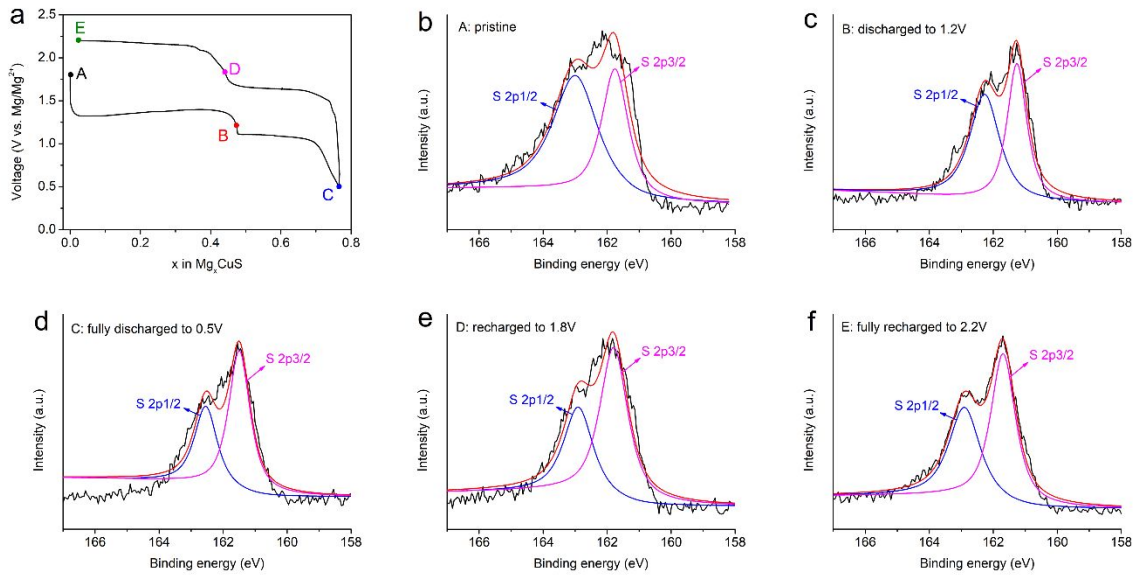

Figure S9. (a) Electrochemical discharge-charge profile of the first cycle showing labeling of the points at which XPS S 2p1/2 spectra were collected. (b-f) S 2p1/2 spectra of CuS at various states during the first cycle.

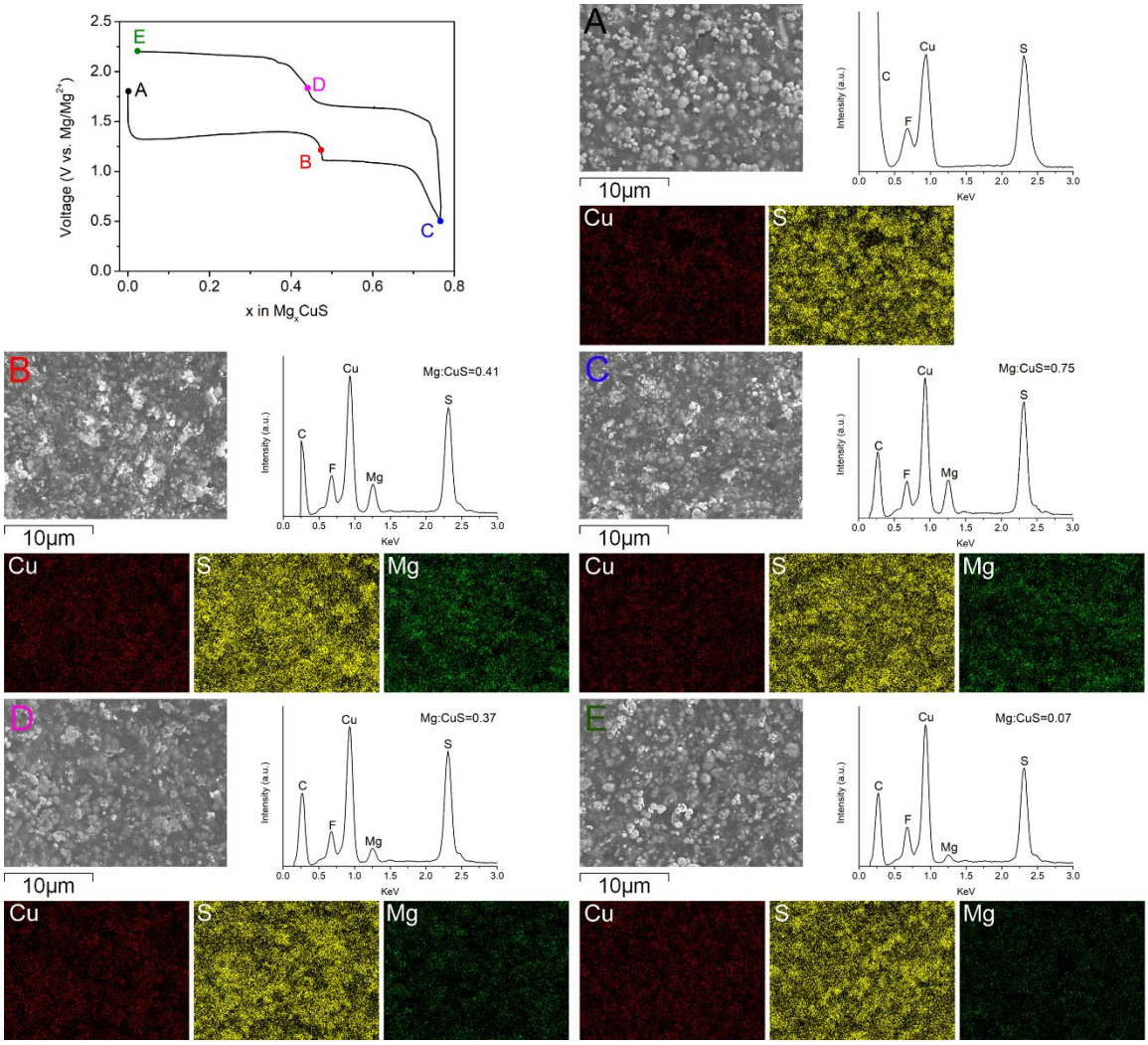

Figure S10. Discharge-charge profile of CuS on the first cycle and EDS spectra of the different discharged/charged states. (A) pristine CuS, (B) Discharged to 1.2V, (C) fully discharged to 0.5V, (D) recharged to 1.8V, and (D) fully recharged to 2.2V.

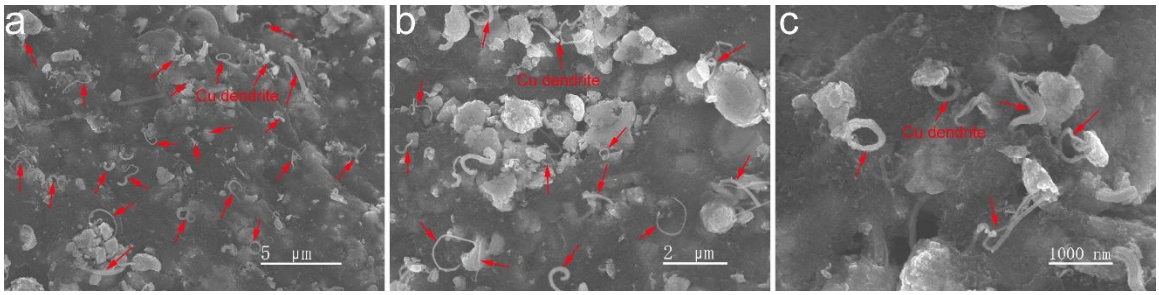

Figure S11. Different-magnification SEM of fully discharged “CuS” electrodes at 0.5V. Cu dendrites are marked with arrows in red.

Certain CuS particles are observed to form Cu dendrite, while some CuS particles without dendrite, which might be due to some Cu dendrite buried into electrodes and not observed. In addition, the discharged capacity of CuS (430 mA h/g) is less than the theoretical one (560 mA h/g). Some CuS particles are not fully reduced to Cu dendrites.

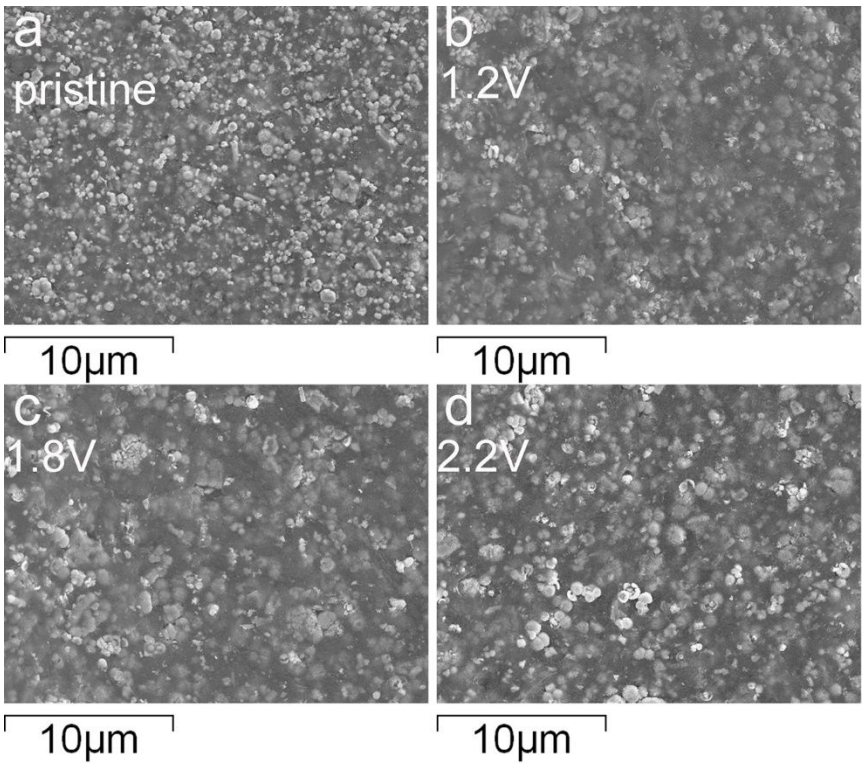

Figure S12. SEM of CuS electrodes at various discharge/charge states: (a) pristine, (b) discharged to 1.2V, (c) recharged to 1.8V, and (d) fully recharged to 2.2V. No Cu dendrite is found at all these electrodes.

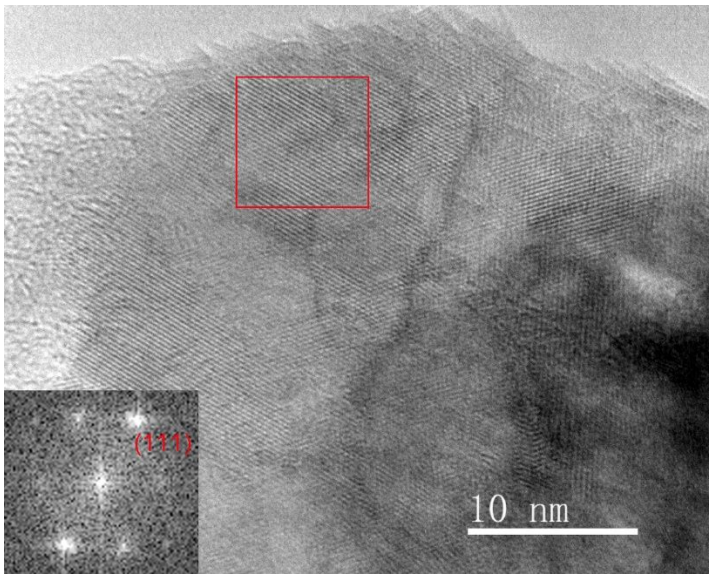

Figure S13. HRTEM and FFT of MgS.

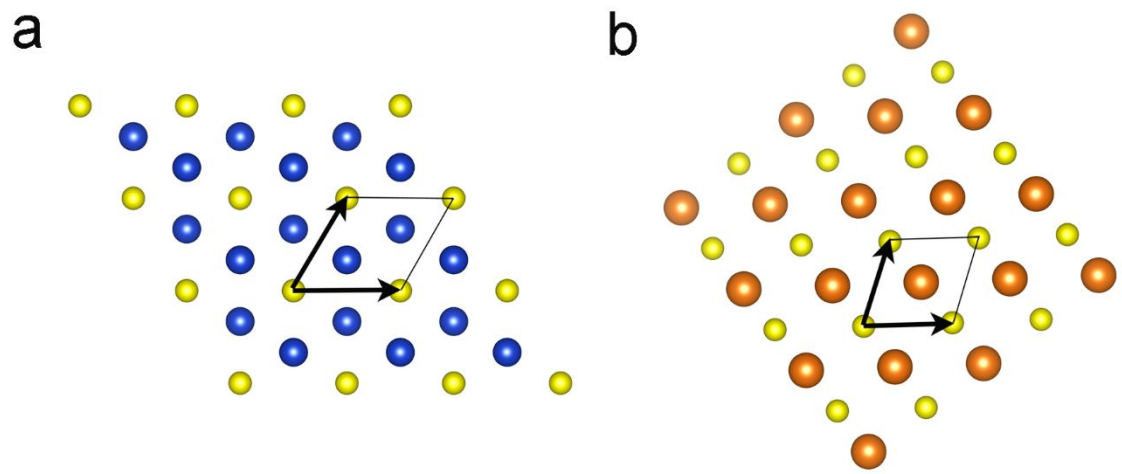

Figure S14. The projected structure of (a) CuS along [001] directions, and (b) MgS along [110] directions. Blue, orange, and yellow balls represent copper, magnesium, and sulfur atoms, respectively.

Reference

1. Doe, R. E.; Han, R.; Hwang, J.; Gmitter, A. J.; Shterenberg, I.; Yoo, H. D.; Pour, N.; Aurbach, D. Novel, electrolyte solutions comprising fully inorganic salts with high anodic stability for rechargeable magnesium batteries. *Chem. Commun.* ***50***, 243-245 (2014).
2. Kubaschewski, O.; Alcock, C.; Spencer, P. Materials thermochemistry. (1993).
3. Chase, M. J Phys Chem Ref Data, Monograph. *American Institute of Physics, Woodbury, NY*, (1998).
4. Mizrahi, O.; Amir, N.; Pollak, E.; Chusid, O.; Marks, V.; Gottlieb, H.; Larush, L.; Zinigrad, E.; Aurbach, D. Electrolyte Solutions with a Wide Electrochemical Window for Rechargeable Magnesium Batteries. ***155***, A103-A109 (2008).
5. Yoo, H. D.; Shterenberg, I.; Gofer, Y.; Gershinsky, G.; Pour, N.; Aurbach, D. Mg rechargeable batteries: an on-going challenge. *Energy Environ. Sci.* ***6***, 2265-2279 (2013).
6. Aurbach, D.; Lu, Z.; Schechter, A.; Gofer, Y.; Gizbar, H.; Turgeman, R.; Cohen, Y.; Moshkovich, M.; Levi, E. Prototype systems for rechargeable magnesium batteries. *Nature* ***407***, 724 (2000).
7. Sun, X.; Bonnick, P.; Duffort, V.; Liu, M.; Rong, Z.; Persson, K. A.; Ceder, G.; Nazar, L. F. A high capacity thiospinel cathode for Mg batteries. *Energy & Environmental Science* ***9***, 2273-2277 (2016).
8. Sun, X.; Bonnick, P.; Nazar, L. F. Layered TiS2 Positive Electrode for Mg Batteries. *ACS Energy Letters* ***1***, 297-301 (2016).
9. Gu, Y.; Katsura, Y.; Yoshino, T.; Takagi, H.; Taniguchi, K. Rechargeable magnesium-ion battery based on a TiSe2-cathode with d-p orbital hybridized electronic structure. *Scientific Reports* ***5***, 12486 (2015).
10. Kouji, T.; Yunpeng, G.; Yukari, K.; Takafumi, Y.; Hidenori, T. Rechargeable Mg battery cathode TiS 3 with d–p orbital hybridized electronic structures. *Applied Physics Express* ***9***, 011801 (2016).
11. Tashiro, Y.; Taniguchi, K.; Miyasaka, H. Copper Selenide as a New Cathode Material based on Displacement Reaction for Rechargeable Magnesium Batteries. *Electrochimica Acta* ***210***, 655-661 (2016).
12. Duffort, V.; Sun, X.; Nazar, L. F. Screening for positive electrodes for magnesium batteries: a protocol for studies at elevated temperatures. *Chemical Communications* ***52***, 12458-12461 (2016).
13. Xiong, F.; Fan, Y.; Tan, S.; Zhou, L.; Xu, Y.; Pei, C.; An, Q.; Mai, L. Magnesium Storage Performance and Mechanism of CuS Cathode. *Nano Energy*, (2018).
14. Choi, J. W.; Aurbach, D. Promise and reality of post-lithium-ion batteries with high energy densities. *Nature Reviews Materials* ***1***, 16013 (2016).